New Target for Cosmic Axion Searches

Daniel Baumann,[1,2,*] Daniel Green,[3,4,†] and Benjamin Wallisch[1,‡]

[1] *DAMTP, University of Cambridge, Cambridge, CB3 0WA, United Kingdom*
[2] *IoP, University of Amsterdam, Amsterdam, 1090 GL, Netherlands*
[3] *Department of Physics, University of California, Berkeley, CA 94720, USA*
[4] *Canadian Institute for Theoretical Astrophysics, Toronto, ON M5S 3H8, Canada*

Future cosmic microwave background experiments have the potential to probe the density of relativistic species at the subpercent level. This sensitivity allows light thermal relics to be detected up to arbitrarily high decoupling temperatures. Conversely, the absence of a detection would require extra light species never to have been in equilibrium with the Standard Model. In this Letter, we exploit this feature to demonstrate the sensitivity of future cosmological observations to the couplings of axions to photons, gluons and charged fermions. In many cases, the constraints achievable from cosmology will surpass existing bounds from laboratory experiments and astrophysical observations by orders of magnitude.

Introduction.—Most of what we know about the history of the universe comes from the observations of light emitted at or after recombination. To learn about earlier times we rely either on theoretical extrapolations or the observations of relics that are left over from an earlier period. One of the most remarkable results of the Planck satellite is the detection of free-streaming cosmic neutrinos [1–3], with an energy density that is consistent with the predicted freeze-out abundance created one second after the Big Bang. Probing even earlier times requires detecting new particles that are more weakly coupled than neutrinos. Such particles arise naturally in many extensions of the Standard Model (SM) [4, 5]. Particularly well-motivated are Goldstone bosons created by the spontaneous breaking of additional global symmetries.

Goldstone bosons are either massless (if the broken symmetry was exact) or naturally light (if it was approximate). Examples of light pseudo-Nambu-Goldstone bosons (pNGBs) are *axions* [6–8], *familons* [9–11], and *majorons* [12, 13], associated with spontaneously broken Peccei-Quinn, family and lepton-number symmetry, respectively. Below the scale of the spontaneous symmetry breaking, the couplings of the Goldstone bosons ϕ to the SM degrees of freedom can be characterized through a set of effective interactions

$$\frac{\mathcal{O}_\phi \mathcal{O}_{\rm SM}}{\Lambda^\Delta}\,, \tag{1}$$

where Λ is related to the symmetry breaking scale. Axion, familon and majoron models are characterized by different couplings in (1). These couplings are constrained by laboratory experiments [5, 14], by astrophysics [15, 16] and by cosmology [17, 18]. While laboratory constraints have the advantage of being direct measurements, their main drawback is that they are usually rather model-specific and sensitive only to narrow windows of pNGB masses. Astrophysical and cosmological constraints are complimentary since they are relatively insensitive to the detailed form of the couplings to the SM and span a wide range of masses. The main astrophysical constraints on new light particles come from stellar cooling [15]. In order not to disrupt successful models of stellar evolution, any new light particles must be more weakly coupled than neutrinos. Moreover, since neutrinos couple to the rest of the SM through a dimension-six operator (suppressed by the electroweak scale), the constraints on extra particles are particularly severe for dimension-four and dimension-five couplings to the SM.

In this Letter, we will show that cosmology is remarkably sensitive to extra light particles. This is because interactions like Eq. (1) can bring these particles into equilibrium with the SM particles. Moreover, thermal equilibrium is democratic. Any new light field that was in thermal equilibrium in the past will have a number density that is comparable to that of photons. This is why neutrinos have been detected with high significance in the CMB [1–3] despite their weak coupling. Like astrophysical constraints, cosmology therefore requires any new light particles to be more weakly coupled than neutrinos. Given the Moore's law-like improvements in CMB detector sensitivity [19, 20], cosmology will push the sensitivity to new light particles beyond the strength of weak scale interactions and has the potential to explore a fundamentally new territory of physics beyond the SM.

Preliminaries.—The total energy density in relativistic species is often defined as

$$\rho_r = \left[1 + \frac{7}{8}\left(\frac{4}{11}\right)^{4/3} N_{\rm eff}\right]\rho_\gamma\,, \tag{2}$$

where ρ_γ is the energy density of photons and the parameter $N_{\rm eff}$ is called the effective number of neutrinos, although there may be contributions that have nothing to do with neutrinos (see e.g. Ref. [21]). The SM predicts $N_{\rm eff} = 3.046$ from neutrinos [22] and the current constraint from the Planck satellite is $N_{\rm eff} = 3.04 \pm 0.18$ [1]. Figure 1 shows the extra contribution to the radiation density of a thermally-decoupled Goldstone boson as a function of its freeze-out temperature T_F. We see that

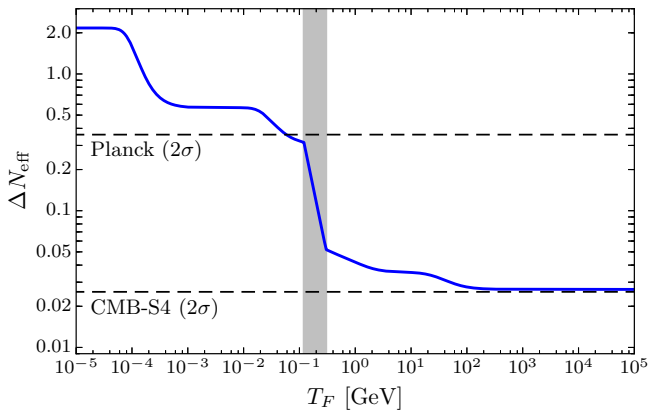

Figure 1. Contribution of a single thermally-decoupled Goldstone boson to the effective number of neutrinos, $\Delta N_{\rm eff}$, as a function of the freeze-out temperature T_F. Shown are also the current 2σ sensitivity of the Planck satellite [1] and an (optimistic) estimate of the sensitivity of a future CMB-S4 mission [3]. The gray band indicates the QCD phase transition.

particles that decoupled *after* the QCD phase transition are effectively ruled out by the observations of the Planck satellite [17]. On the other hand, the effect of particles that decoupled *before* the QCD phase transition is suppressed by an order of magnitude, $0.05 \geq \Delta N_{\rm eff} \geq 0.027$. Although Planck is blind to these particles, this regime is within reach of future experiments. In particular, the planned CMB Stage IV (CMB-S4) experiments have the potential to constrain (or detect) extra relativistic species at the level of $\sigma(N_{\rm eff}) \sim 0.01$ [3, 19, 20]. To simplify the narrative, we will assume that the sensitivity to $\Delta N_{\rm eff} = 0.027$ will be reached with CMB-S4, either on its own or in conjunction with other data [23, 24]. Alternatively, our arguments could be viewed as strong motivation for reaching this critical level of sensitivity in future experiments.

Future CMB constraints.—Even the absence of a detection would be very informative, because it would strongly constrain the couplings between the extra light relics and the SM degrees of freedom. This is because a thermal abundance can be avoided if the reheating temperature of the universe, T_R, is below the would-be freeze-out temperature, i.e. $T_R < T_F$. In that case, the extra particles have never been in thermal equilibrium and their densities therefore do not have to be detectable. In the absence of a detection, requiring $T_F(\Lambda) > T_R$ would place very strong bounds on the scale(s) in Eq. (1), i.e. $\Lambda > T_F^{-1}(T_R)$. We note that these constraints make no assumption about the nature of dark matter because the thermal population of axions arises independently of a possible cold population. On the other hand, we have to assume that the effective description of the pNGBs with interactions of the form of Eq. (1) holds up to $T_F \ll \Lambda$. This is equivalent to assuming that the UV completion of the effective theory is not too weakly coupled. Moreover, we also require the absence of any significant dilution of $\Delta N_{\rm eff}$ after freeze-out. In practice, this means that we are restricting to scenarios with $\Delta g_*(T_F) \lesssim g_*^{\rm SM}(T_F) \approx 10^2$. Finally, our results will be restricted to $m_\phi < 1\,\text{MeV}$, so that the only possible decays of the pNGBs are to photons or neutrinos. In the remainder, we will derive future CMB constraints on the couplings of pNGBs to SM gauge fields (for axions) and charged fermions (for familons). Similar bounds for the couplings to neutrinos (for majorons) can be found in Refs. [25–27].

Constraints on axions.—Axions arise naturally in many areas of high-energy physics, the QCD axion being a particularly well-motivated example. They are a compelling example of a new particle that is experimentally elusive [5, 14] because of its weak coupling rather than due to kinematic constraints. What typically distinguishes axions from other pNGBs are their unique couplings to the SM gauge fields. Below the scale of electroweak symmetry breaking (EWSB), we consider the following effective theory with shift-symmetric couplings of the axion:

$$\mathcal{L}_{\phi\rm EW} = -\frac{1}{4}\left(\frac{\phi}{\Lambda_\gamma} F_{\mu\nu}\tilde{F}^{\mu\nu} + \frac{\phi}{\Lambda_g} G^a_{\mu\nu}\tilde{G}^{\mu\nu,a}\right), \quad (3)$$

where $X_{\mu\nu} \equiv \{F_{\mu\nu}, G^a_{\mu\nu}\}$ are the field strengths for the photons and gluons, and $\tilde{X}^{\mu\nu} \equiv \frac{1}{2}\epsilon^{\mu\nu\rho\sigma}X_{\rho\sigma}$ are their duals. Axion models will typically include couplings to all SM gauge fields, but only the coupling to gluons is strictly necessary to solve the strong CP problem. At high energies, the rate of axion production through the gauge field interactions can be expressed as [28] (see also Refs. [29–32])

$$\Gamma(\Lambda_n, T) = \sum_n \gamma_n(T)\,\frac{T^3}{\Lambda_n^2}\,. \quad (4)$$

The prefactors $\gamma_n(T)$ have their origin in the running of the couplings and are only weakly dependent on temperature. For simplicity of presentation, we will treat these functions as constants, but take them into account in Ref. [33]. We see that the production rate, $\Gamma \propto T^3$, decreases faster than the expansion rate during the radiation era, $H \propto T^2$. The axions therefore *freeze out* when the production rate drops below the expansion rate, with the freeze-out temperature T_F determined by $\Gamma(T_F) = H(T_F)$. To avoid this thermal axion abundance requires $T_F > T_R$, or

$$\Gamma(\Lambda_n, T_R) < H(T_R) = \frac{\pi}{\sqrt{90}}\sqrt{g_{*,R}}\,\frac{T_R^2}{M_{\rm pl}}\,, \quad (5)$$

where $M_{\rm pl}$ is the reduced Planck mass and $g_{*,R} \equiv g_*(T_R)$ denotes the effective number of relativistic species at T_R.

For a given reheating temperature, this is a constraint on the couplings Λ_n in Eq. (4). Treating the different axion couplings separately, we can write

$$\Lambda_n \;>\; \left(\frac{\pi^2}{90} g_{*,R}\right)^{-1/4} \sqrt{\gamma_{n,R} T_R M_{\rm pl}}\,, \tag{6}$$

where $\gamma_{n,R} \equiv \gamma_n(T_R)$.

The operator that has been most actively investigated experimentally is the coupling to photons. Photons are easily produced in large numbers in both the laboratory and in many astrophysical settings which makes this coupling a particularly fruitful target for axion searches. The electroweak couplings in the high-energy theory prior to EWSB are related to the photon coupling Λ_γ through the Weinberg mixing angle. In [33], we show in detail how the constraints (6) on the couplings to the electroweak gauge bosons map into a constraint on the coupling to photons. This constraint is a function of the relative size of the couplings to the $SU(2)_L$ and $U(1)_Y$ sectors. To be conservative, we will here present the weakest constraint which arises when the axion only couples to the $U(1)_Y$ gauge field. A specific axion model is likely to also couple to the $SU(2)_L$ sector and the constraint on Λ_γ would then be stronger (as can be seen explicitly in [33]). Using $\gamma_{\gamma,R} \approx \gamma_\gamma(10^{10}\,\text{GeV}) = 0.029$ and $g_{*,R} = 106.75 + 1$, we find

$$\Lambda_\gamma \;>\; 1.4 \times 10^{13}\,\text{GeV}\,\sqrt{T_{R,10}}\,, \tag{7}$$

where $T_{R,10} \equiv T_R/10^{10}\,\text{GeV}$. For a reheating temperature of about $10^{10}\,\text{GeV}$, the bound in (7) is three orders of magnitude stronger than the best current constraints (cf. Fig. 2). Even for a reheating temperature as low as $10^4\,\text{GeV}$ the bound from the CMB would still marginally improve over existing constraints.

Massive axions are unstable to decay mediated by the operator $\phi F\tilde{F}$. However, for couplings compatible with the stellar cooling constraint, $\Lambda_\gamma > 1.3 \times 10^{10}\,\text{GeV}$ [35], and masses $m_\phi \lesssim 10\,\text{keV}$, these decays occur after recombination and, hence, the axions are effectively stable [33]. The regime $10\,\text{keV} < m_\phi < 1\,\text{MeV}$ (where the axion decays between neutrino decoupling and recombination) is constrained by effects on the CMB and on Big Bang Nucleosynthesis (BBN) [36–38].

The coupling to gluons is especially interesting for the QCD axion since it has to be present in order to solve the strong CP problem. The axion production rate associated with the gluon interaction in Eq. (3) is $\Gamma_g \simeq 0.41 T^3/\Lambda_g^2$ [28]. As before, we have dropped a weakly temperature-dependent prefactor, but account for it in Ref. [33]. The bound (6) then implies

$$\Lambda_g > 5.4 \times 10^{13}\,\text{GeV}\,\sqrt{T_{R,10}}\,. \tag{8}$$

Laboratory constraints on the axion-gluon coupling are usually phrased in terms of the induced electric dipole moment (EDM) of nucleons: $d_n = g_d \phi_0$, where ϕ_0 is the value of the local axion field. The coupling g_d is given for the QCD axion by [39, 40]

$$g_d \;\approx\; \frac{2\pi}{\alpha_s} \times \frac{3.8 \times 10^{-3}\,\text{GeV}^{-1}}{\Lambda_g}\,. \tag{9}$$

Constraints on g_d (and hence Λ_g) are shown in Fig. 3. We see that future CMB-S4 observations will improve over existing constraints on Λ_g by up to six orders of magnitude if $T_R = \mathcal{O}(10^{10}\,\text{GeV})$. Even if the reheating temperature is as low as $10^4\,\text{GeV}$, the future CMB constraints will be tighter by three orders of magnitude.

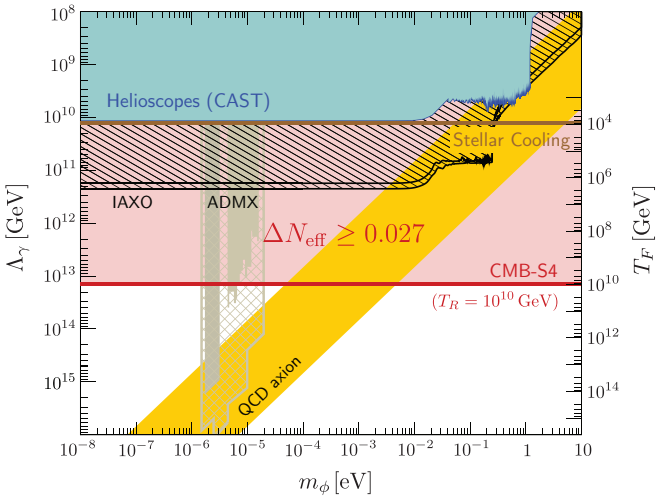

Figure 2. Comparison between current constraints on the axion-photon coupling and the sensitivity of a future CMB-S4 mission (figure adapted from Ref. [34]). Future laboratory constraints (IAXO and ADMX) are shown as shaded regions. The yellow band indicates a range of representative models for the QCD axion. The future CMB bound is a function of the reheating temperature T_R. We note that ADMX assumes that the axion is all of the dark matter, while all other constraints do not have this restriction.

Constraints on familons.—Spontaneously broken global symmetries have also been envoked to explain the approximate $U(3)^5$ flavor symmetry of the Standard Model. The associated pNGBs—called *familons* [9–11]—couple to the SM through Yukawa couplings,

$$\begin{aligned}\mathcal{L}_{\phi\psi} &= -\frac{\partial_\mu \phi}{\Lambda_\psi}\,\bar{\psi}_i \gamma^\mu \left(g_V^{ij} + g_A^{ij}\gamma^5\right)\psi_j \\ &\to \frac{\phi}{\Lambda_\psi}\left(\mathrm{i}H\,\bar{\psi}_{L,i}\left[\sum_{I=V,A}(\lambda_i \mp \lambda_j) g_I^{ij}\right]\psi_{R,j} + \text{h.c.}\right),\end{aligned} \tag{10}$$

where H is the Higgs doublet and $\psi_{L,R} \equiv \frac{1}{2}(1 \mp \gamma^5)\psi$. The $SU(2)_L$ and $SU(3)_c$ structures in Eq. (10) take the same form as for the SM Yukawa couplings [43], but this has been left implicit to avoid clutter. In the sec-

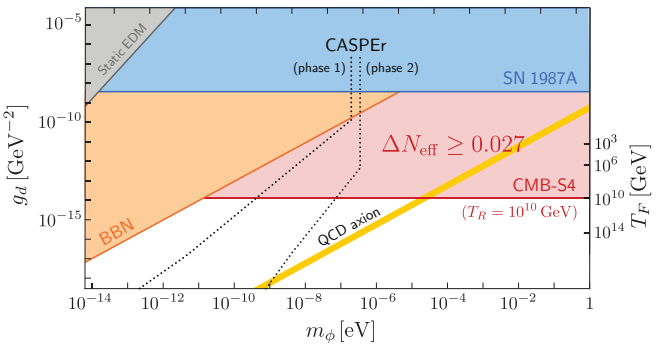

Figure 3. Comparison between current constraints on the axion-gluon coupling and the sensitivity of a future CMB-S4 mission (figure adapted from Refs. [40, 41]). The dotted lines are the projected sensitivities of the NMR experiment CASPEr [42]. We note that CASPEr, the static EDM [40] and BBN constraints [41] assume that the axion is all of the dark matter, while SN 1987A [15] and the future CMB constraint do not have this restriction.

ond line we have integrated by parts and used the equations of motion. The subscripts V and A denote the couplings to the vector and axial-vector currents, respectively, and $\lambda_i \equiv \sqrt{2} m_i/v$ are the Yukawa couplings, with $v = 246\,{\rm GeV}$ being the Higgs vacuum expectation value. We note that the diagonal couplings, $i = j$, are only to the axial part, as expected from vector current conservation. In Table I, we have collected accelerator and astrophysics constraints on the effective couplings $\Lambda^I_{ij} \equiv \Lambda_\psi/g^{ij}_I$ and $\Lambda_{ij} \equiv \Lambda_\psi/[(g^{ij}_V)^2 + (g^{ij}_A)^2]^{1/2}$. We see that current data typically constrain the couplings to the first generation fermions much more than those to the second and third generations. We wish to compare these constraints to the reach of future CMB observations.

Above the EWSB scale, the production of the familon ϕ is determined by a four-point interaction. This allows the following processes: $\bar\psi_i + \psi_j \to H + \phi$ and $\psi_i + H \to \psi_j + \phi$. The total production rate is [33]

$$\Gamma^I_{ij} \simeq 0.37\, N_\psi\, \frac{(\lambda_i \mp \lambda_j)^2}{8\pi}\, \frac{T^3}{(\Lambda^I_{ij})^2}\,, \tag{11}$$

where $N_\psi = 1$ for charged leptons and $N_\psi = 3$ for quarks. The "$-$" and "$+$" signs apply to $I = V$ and $I = A$, respectively. Deriving the freeze-out temperature and imposing $T_F > T_R$, we find

$$\Lambda^I_{ij} > \frac{m_i \mp m_j}{m_{\tau/t}}\, \sqrt{T_{R,10}} \begin{cases} 1.0 \times 10^{11}\,{\rm GeV}\,, \\ \\ 1.8 \times 10^{13}\,{\rm GeV}\,, \end{cases} \tag{12}$$

where the first line applies to charged leptons with $m_\tau \approx 1.8\,{\rm GeV}$ and the second to quarks with $m_t \approx 173\,{\rm GeV}$. In Table I, we show how these bounds compare to current laboratory and astrophysics constraints for a fiducial reheating temperature of $10^{10}\,{\rm GeV}$. Except for the coupling to electrons, the constraints from future CMB experiments are orders of magnitude stronger than existing constraints. For lower reheating temperatures the constraints would weaken proportional to $\sqrt{T_R}$. We note that, except for the top quark, laboratory and astrophysical constraints are considerably weaker for second and third generation particles because of kinematics, while the cosmological constraints are strengthened for the higher mass fermions due to the larger effective strength of the interactions.

Below the EWSB scale, the leading coupling of the familon to fermions becomes marginal after replacing the Higgs in Eq. (10) with its vacuum expectation value. The temperature dependence of the interaction rate is then weaker than that of the Hubble expansion rate, leading to a recoupling (i.e. freeze-in) of the pNGBs at low temperatures. To avoid a large density of pNGBs requires that the freeze-in temperature $T_{\tilde F}$ is smaller than the mass of the fermions participating in the interactions, $T_{\tilde F} < m_\psi$, so that the interaction rate becomes Boltzmann suppressed before freeze-in can occur. Again, this constraint can be expressed as a bound on the scales that couple the pNGBs to the SM fermions.

For the diagonal couplings in Eq. (10), the production rate is dominated by a Compton-like process, $\{\gamma, g\} + \psi_i \to \psi_i + \phi$, and by fermion-antifermion annihilation, $\bar\psi_i + \psi_i \to \{\gamma, g\} + \phi$, where $\{\gamma, g\}$ is either a photon or gluon depending on whether the fermion is a lepton or quark. Since freeze-in occurs at low temperatures, the quark production becomes sensitive to strong coupling effects. We therefore only present bounds for the lepton couplings. Above the lepton mass, the production rate is $\tilde\Gamma_{ii} \simeq 5.3\,\alpha\,|\tilde\epsilon_{ii}|^2/(8\pi)\,T$ [33], where $\tilde\epsilon_{ii} \equiv 2m_i/\Lambda_{ii}$. Deriving the freeze-in temperature and imposing $T_{\tilde F} < m_i$, we find

$$\Lambda_{ii} > 9.5 \times 10^7\,{\rm GeV} \left(\frac{g_{*,\tau}}{g_{*,i}}\right)^{1/4} \left(\frac{\alpha_i}{\alpha_\tau}\,\frac{m_i}{m_\tau}\right)^{1/2}\,, \tag{13}$$

where $g_{*,i}$ and α_i are the effective number of relativistic species and the fine-structure constant at $T = m_i$. Except for the coupling to electrons, these new bounds are significantly stronger than the existing constraints. In particular, it is worth noting that the Planck constraint on the diagonal muon coupling, $\Lambda_{\mu\mu} > 3.4 \times 10^7\,{\rm GeV}$, improves on the current experimental bound by more than an order of magnitude.

For the off-diagonal couplings in Eq. (10), we have the possibility of a freeze-in population of the familon from the decay of the heavy fermion, $\psi_i \to \psi_j + \phi$. For $m_i \gg m_j$, the production rate associated with this process is $\tilde\Gamma_{ij} \simeq 0.31\, N_\psi\, |\tilde\epsilon_{ij}|^2/(8\pi)\, m_i^2/T$ [33], where $\tilde\epsilon_{ij} \approx m_i/\Lambda_{ij}$. Requiring the corresponding freeze-in temperature to be

	Current Constraints		Future CMB Constraints		
Coupling	Bound [GeV]	Origin	Freeze-Out [GeV]	Freeze-In [GeV]	$\Delta\tilde{N}_{\rm eff}$
Λ_{ee}	1.2×10^{10}	White dwarfs	6.0×10^{7}	2.7×10^{6}	1.3
$\Lambda_{\mu\mu}$	2.0×10^{6}	Stellar cooling	1.2×10^{10}	3.4×10^{7}	0.5
$\Lambda_{\tau\tau}$	2.5×10^{4}	Stellar cooling	2.1×10^{11}	9.5×10^{7}	0.05
Λ_{bb}	6.1×10^{5}	Stellar cooling	9.5×10^{11}	$\cdots$	0.04
Λ_{tt}	1.2×10^{9}	Stellar cooling	3.5×10^{13}	$\cdots$	0.03
$\Lambda^{V}_{\mu e}$	5.5×10^{9}	$\mu^+\to e^+\,\phi$	6.2×10^{9}	4.8×10^{7}	0.5
$\Lambda_{\mu e}$	3.1×10^{9}	$\mu^+\to e^+\,\phi\,\gamma$	6.2×10^{9}	4.8×10^{7}	0.5
$\Lambda_{\tau e}$	4.4×10^{6}	$\tau^-\to e^-\phi$	1.0×10^{11}	1.3×10^{8}	0.05
$\Lambda_{\tau\mu}$	3.2×10^{6}	$\tau^-\to \mu^-\phi$	1.0×10^{11}	1.3×10^{8}	0.05
Λ^{A}_{cu}	6.9×10^{5}	D^0-$\bar{D}^0$	1.3×10^{11}	2.0×10^{8}	0.05
Λ^{A}_{bd}	6.4×10^{5}	B^0-$\bar{B}^0$	4.8×10^{11}	3.7×10^{8}	0.04
Λ_{bs}	6.1×10^{7}	$b\to s\phi$	4.8×10^{11}	3.7×10^{8}	0.04
Λ_{tu}	6.6×10^{9}	Mixing	1.8×10^{13}	2.1×10^{9}	0.03
Λ_{tc}	2.2×10^{9}	Mixing	1.8×10^{13}	2.1×10^{9}	0.03

Table I. Current experimental constraints on Goldstone-fermion couplings [17, 44, 45] and future CMB constraints. The quoted freeze-out bounds are for $T_R = 10^{10}\,\text{GeV}$ and require that a future CMB experiment excludes $\Delta N_{\rm eff} = 0.027$. The freeze-in bounds, in contrast, do not depend on T_R and assume weaker exclusions $\Delta\tilde{N}_{\rm eff}$ [see the last column for estimates of the freeze-in contributions associated with the different couplings, $\Delta\tilde{N}_{\rm eff}\approx\Delta N_{\rm eff}(\frac{1}{4}m_i)$].

below the mass of the heavier fermion, $T_{\bar{F}} < m_i$, we get

$$\Lambda_{ij} > \left(\frac{g_{*,\tau/t}}{g_{*,i}}\right)^{1/4}\left(\frac{m_i}{m_{\tau/t}}\right)^{1/2}\begin{cases}1.3\times10^{8}\,\text{GeV}\,,\\ 2.1\times10^{9}\,\text{GeV}\,,\end{cases} \tag{14}$$

where the first line applies to charged leptons and the second to quarks. We see that this improves over existing constraints for the third generation leptons and for the second and third generation quarks (except the top).

Conclusions.—In closing, we would like to re-emphasize that $\Delta N_{\rm eff} = 0.027$ is an important theoretical threshold (see Refs. [17, 28, 46, 47] for related discussions). Remarkably, this target is within reach of future cosmological observations [23], including the planned CMB-S4 mission [19]. These observations therefore have the potential to probe for light thermal relics up to arbitrarily high decoupling temperatures. We consider this to be a unique opportunity to detect new particles, or place very strong constraints on their couplings to the Standard Model.

We thank Jens Chluba, Nathaniel Craig, Daniel Grin, Julien Lesgourgues, David Marsh, Joel Meyers and Surjeet Rajendran for helpful discussions. D. G. and B. W. thank the Institute of Physics at the University of Amsterdam for its hospitality. D. B. and B. W. acknowledge support from a Starting Grant of the European Research Council (ERC STG Grant 279617). B. W. is also supported by a Cambridge European Scholarship of the Cambridge Trust and an STFC Studentship. D. G. was supported by an NSERC Discovery Grant and the Canadian Institute for Advanced Research.

* dbaumann@damtp.cam.ac.uk
† drgreen@cita.utoronto.ca
‡ b.wallisch@damtp.cam.ac.uk

[1] P. Ade *et al.* (Planck Collaboration), Astron. Astrophys. **594**, A13 (2016).
[2] B. Follin, L. Knox, M. Millea, and Z. Pan, Phys. Rev. Lett. **115**, 091301 (2015).
[3] D. Baumann, D. Green, J. Meyers, and B. Wallisch, J. Cosmol. Astropart. Phys. **1601**, 007 (2016).
[4] J. Jaeckel and A. Ringwald, Annu. Rev. Nucl. Part. Sci. **60**, 405 (2010).
[5] R. Essig *et al.*, arXiv:1311.0029 [hep-ph].
[6] R. Peccei and H. Quinn, Phys. Rev. Lett. **38**, 1440 (1977).
[7] S. Weinberg, Phys. Rev. Lett. **40**, 223 (1978).
[8] F. Wilczek, Phys. Rev. Lett. **40**, 279 (1978).
[9] F. Wilczek, Phys. Rev. Lett. **49**, 1549 (1982).
[10] D. Reiss, Phys. Lett. B **115**, 217 (1982).
[11] J. Kim, Phys. Rep. **150**, 1 (1987).
[12] Y. Chikashige, R. Mohapatra, and R. Peccei, Phys. Lett. B **98**, 265 (1981).
[13] Y. Chikashige, R. Mohapatra, and R. Peccei, Phys. Rev. Lett. **45**, 1926 (1980).
[14] P. Graham, I. Irastorza, S. Lamoreaux, A. Lindner, and K. van Bibber, Ann. Rev. Nucl. Part. Sci. **65**, 485 (2015).
[15] G. Raffelt, *Stars as Laboratories for Fundamental Physics* (University of Chicago Press, Chicago, IL, 1996).
[16] G. Raffelt, Proc. Int. Sch. Phys. Fermi **182**, 61 (2012).
[17] C. Brust, D. Kaplan, and M. Walters, J. High Energy Phys. **12**, 058 (2013).
[18] D. Marsh, Phys. Rep. **643**, 1 (2016).
[19] K. Abazajian *et al.*, Astropart. Phys. **63**, 66 (2015).
[20] W. Wu *et al.*, Astrophys. J. **788**, 138 (2014).
[21] S. Weinberg, Phys. Rev. Lett. **110**, 241301 (2013).

[22] G. Mangano, G. Miele, S. Pastor, T. Pinto, O. Pisanti, and P. Serpico, Nucl. Phys. B **729**, 221 (2005).

[23] A. Font-Ribera, P. McDonald, N. Mostek, B. Reid, H.-J. Seo, and A. Slosar, J. Cosmol. Astropart. Phys. **1405**, 023 (2014).

[24] A. Manzotti, S. Dodelson, and Y. Park, Phys. Rev. D **93**, 063009 (2016).

[25] Z. Chacko, L. Hall, T. Okui, and S. Oliver, Phys. Rev. D **70**, 085008 (2004).

[26] S. Hannestad and G. Raffelt, Phys. Rev. D **72**, 103514 (2005).

[27] A. Friedland, K. Zurek, and S. Bashinsky, arXiv:0704.3271 [astro-ph].

[28] A. Salvio, A. Strumia, and W. Xue, J. Cosmol. Astropart. Phys. **1401**, 011 (2014).

[29] E. Braaten and T. Yuan, Phys. Rev. Lett. **66**, 2183 (1991).

[30] M. Bolz, A. Brandenburg, and W. Buchmüller, Nucl. Phys. B **606**, 518 (2001).

[31] E. Masso, F. Rota, and G. Zsembinszki, Phys. Rev. D **66**, 023004 (2002).

[32] P. Graf and F. Steffen, Phys. Rev. D **83**, 075011 (2011).

[33] See Supplemental Material for derivations of the pNGB production rates and a discussion of the (negligible) effects of decays of pNGBs on the derived bounds.

[34] G. Carosi, A. Friedland, M. Giannotti, M. Pivovaroff, J. Ruz, and J. Vogel, arXiv:1309.7035 [hep-ph].

[35] A. Friedland, M. Giannotti, and M. Wise, Phys. Rev. Lett. **110**, 061101 (2013).

[36] D. Cadamuro, S. Hannestad, G. Raffelt, and J. Redondo, J. Cosmol. Astropart. Phys. **1102**, 003 (2011).

[37] D. Cadamuro and J. Redondo, J. Cosmol. Astropart. Phys. **1202**, 032 (2012).

[38] M. Millea, L. Knox, and B. Fields, Phys. Rev. D **92**, 023010 (2015).

[39] M. Pospelov and A. Ritz, Phys. Rev. Lett. **83**, 2526 (1999).

[40] P. Graham and S. Rajendran, Phys. Rev. D **88**, 035023 (2013).

[41] K. Blum, R. D'Agnolo, M. Lisanti, and B. Safdi, Phys. Lett. B **737**, 30 (2014).

[42] D. Budker, P. Graham, M. Ledbetter, S. Rajendran, and A. Sushkov, Phys. Rev. X **4**, 021030 (2014).

[43] M. Peskin and D. Schroeder, *An Introduction to Quantum Field Theory* (Addison-Wesley, Reading, MA, 1995).

[44] J. Feng, T. Moroi, H. Murayama, and E. Schnapka, Phys. Rev. D **57**, 5875 (1998).

[45] B. Hansen, H. Richer, J. Kalirai, R. Goldsbury, S. Frewen, and J. Heyl, Astrophys. J. **809**, 141 (2015).

[46] M. Kawasaki, M. Yamada, and T. Yanagida, Phys. Rev. D **91**, 125018 (2015).

[47] Z. Chacko, Y. Cui, S. Hong, and T. Okui, Phys. Rev. D **92**, 055033 (2015).

Supplemental Material: New Target for Cosmic Axion Searches

Daniel Baumann,[1,2] Daniel Green,[3,4] and Benjamin Wallisch[1]

[1] *DAMTP, University of Cambridge, Cambridge, CB3 0WA, United Kingdom*
[2] *IoP, University of Amsterdam, Amsterdam, 1090 GL, Netherlands*
[3] *Department of Physics, University of California, Berkeley, CA 94720, USA*
[4] *Canadian Institute for Theoretical Astrophysics, Toronto, ON M5S 3H8, Canada*

This document contains material supplementary to our letter *New Target for Cosmic Axion Searches*. In the first part, we derive the rates of Goldstone boson production that were used to obtain the results of the letter. In the second part, we discuss the (negligible) effects of decays of the massive Goldstone bosons on the derived bounds.

PRODUCTION RATES

In this part, we derive the rates of Goldstone boson production used in the main text. We consider separately the couplings to gauge fields and to matter fields.

Couplings to Gauge Fields

Above the scale of electroweak symmetry breaking (EWSB), the coupling of the Goldstone boson to the Standard Model (SM) gauge sector is

$$\mathcal{L}_\phi = -\frac{1}{4}\frac{\phi}{\Lambda}\Big(c_1\, B_{\mu\nu}\tilde{B}^{\mu\nu} + c_2\, W^a_{\mu\nu}\tilde{W}^{\mu\nu,a} + c_3\, G^a_{\mu\nu}\tilde{G}^{\mu\nu,a}\Big)\,. \tag{S1}$$

The Goldstone production associated with the couplings in (S1) was considered in [S1–S5]. In the limit of massless gauge bosons, the cross sections for some of the processes have infrared (IR) divergences, and the results depend slightly on how these divergences are regulated. In [S5], the total production rate was found to be

$$\Gamma = \frac{T^3}{8\pi\Lambda^2}\Big[c_1^2\, F_1(T) + 3c_2^2\, F_2(T) + 8c_3^2\, F_3(T)\Big]\,, \tag{S2}$$

where the functions $F_n(T)$ were derived numerically. We extracted $F_n(T)$ from Fig. 1 of [S5], together with the one-loop running of the gauge couplings $\alpha_i(T)$.

Coupling to gluons.—To isolate the effect of the coupling to gluons, we write $c_1 = c_2 \equiv 0$ and define $\Lambda_g \equiv \Lambda/c_3$. The production rate (S2) then becomes

$$\Gamma_g(T) = \frac{F_3(T)}{\pi}\frac{T^3}{\Lambda_g^2} \equiv \gamma_g(T)\frac{T^3}{\Lambda_g^2}\,, \tag{S3}$$

where $\gamma_g(10^{10}\,\text{GeV}) = 0.41$. The function $\gamma_g(T)$ is presented in the left panel of Fig. S1. The freeze-out bound on the gluon coupling then is

$$\Lambda_g > \left(\frac{\pi^2}{90}g_{*,R}\right)^{-1/4}\sqrt{\gamma_{g,R}\,T_R\,M_{\rm pl}} \equiv \lambda_g(T_R)\left(\frac{T_R}{10^{10}\,\text{GeV}}\right)^{1/2}, \tag{S4}$$

where $g_{*,R} \equiv g_*(T_R)$ and $\gamma_{g,R} \equiv \gamma_g(T_R)$. The bound in (S4) is illustrated in the right panel of Fig. S1. In the main text, we used $\lambda_g(10^{10}\,\text{GeV}) = 5.4\times10^{13}\,\text{GeV}$.

Coupling to photons.—To isolate the coupling to the electroweak sector, we set $c_3 = 0$. In this case, the Lagrangian (S1) can be written as

$$\mathcal{L}_\phi = -\frac{1}{4}\frac{\phi}{\Lambda}\left(c_a\, B_{\mu\nu}\tilde{B}^{\mu\nu} + s_a\, W^a_{\mu\nu}\tilde{W}^{\mu\nu,a}\right)\,, \tag{S5}$$

where we have defined

$$\Lambda \to \frac{\Lambda}{\sqrt{c_1^2+c_2^2}}\,,\quad c_a \equiv \frac{c_1}{\sqrt{c_1^2+c_2^2}}\,,\quad s_a \equiv \frac{c_2}{\sqrt{c_1^2+c_2^2}}\,. \tag{S6}$$

Note that $c_a^2 + s_a^2 = 1$, so we can use Λ and c_a as the two free parameters. The production rate (S2) is then given by

$$\Gamma = \frac{[c_a^2 F_1(T) + 3s_a^2\, F_2(T)]}{8\pi}\frac{T^3}{\Lambda^2} \equiv \gamma(T, c_a)\,\frac{T^3}{\Lambda^2}\,. \tag{S7}$$

The function $\gamma(T, c_a)$ is shown in the left panel of Fig. S2. In the main text, we employed $\gamma(10^{10}\,\text{GeV}, 1) = 0.017$. The freeze-out bound on the coupling then is

$$\Lambda(c_a) > \left(\frac{\pi^2}{90}g_{*,R}\right)^{-1/4}\sqrt{\gamma_R(c_a)\,T_R\,M_{\rm pl}}\,, \tag{S8}$$

where $\gamma_R(c_a) \equiv \gamma(T_R, c_a)$. We wish to relate this bound to the couplings below the EWSB scale.

At low energies, the axion couplings to the electroweak sector become

$$\mathcal{L}_{\phi\rm EW} = -\frac{1}{4}\left(\frac{\phi}{\Lambda_\gamma}F_{\mu\nu}\tilde{F}^{\mu\nu} + \frac{\phi}{\Lambda_Z}Z_{\mu\nu}\tilde{Z}^{\mu\nu} + \frac{\phi}{\Lambda_{Z\gamma}}Z_{\mu\nu}\tilde{F}^{\mu\nu} + \frac{\phi}{\Lambda_W}W^+_{\mu\nu}\tilde{W}^{-\mu\nu}\right), \tag{S9}$$

where $F_{\mu\nu}$, $Z_{\mu\nu}$ and $W^\pm_{\mu\nu}$ are the field strengths for the photon, Z and $W^\pm$, respectively. Here, we have dropped additional (non-Abelian) terms proportional to c_2 which are cubic in the gauge fields. In order to match the high-energy couplings in (S5) to the low-energy couplings

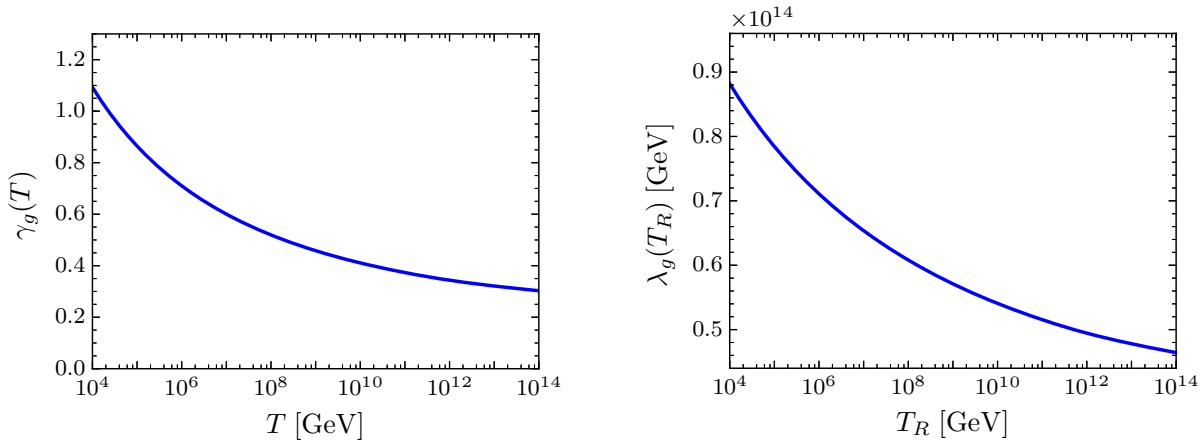

Figure S1. *Left*: Axion production rate associated with the coupling to gluons as parametrized by $\gamma_g(T)$ in (S3). *Right*: Constraint on the axion-gluon coupling Λ_g as parametrized by $\lambda_g(T_R)$ in (S4).

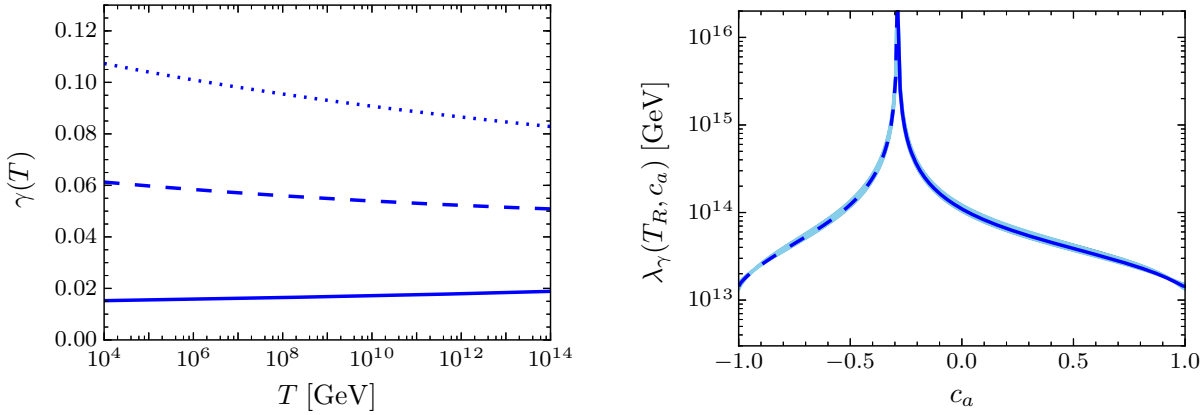

Figure S2. *Left*: Axion production rate associated with the coupling to the electroweak gauge bosons as parametrized by $\gamma(T, c_a)$ in (S7) for $c_a = 0$ (dotted line), $1/\sqrt{2}$ (dashed line) and 1 (solid line). *Right*: Constraint on the axion-photon coupling Λ_γ as parametrized by $\lambda_\gamma(T_R, c_a)$ in (S14). The solid and dashed lines correspond to bounds on positive and negative Λ_γ for $T_R = 10^{10}\,\text{GeV}$. The band displays the change for reheating temperatures between $10^4\,\text{GeV}$ (upper edge) and $10^{15}\,\text{GeV}$ (lower edge).

in (S9), we define

$$\Lambda_\gamma^{-1} = \left(c_w^2\, c_a + s_w^2\, s_a\right) \Lambda^{-1}\,, \tag{S10}$$

$$\Lambda_Z^{-1} = \left(c_w^2\, s_a + s_w^2\, c_a\right) \Lambda^{-1}\,, \tag{S11}$$

$$\Lambda_{Z\gamma}^{-1} = 2 s_w c_w\, (s_a - c_a)\, \Lambda^{-1}\,, \tag{S12}$$

$$\Lambda_W^{-1} = s_a\, \Lambda^{-1}\,, \tag{S13}$$

where $\{c_w, s_w\} \equiv \{\cos\theta_w, \sin\theta_w\}$, with $\theta_w \approx 30^\circ$ the Weinberg mixing angle. Using (S10), we can write (S8) as a bound on the photon coupling,

$$\begin{aligned}\Lambda_\gamma(c_a) &> \frac{1}{c_w^2\, c_a + s_w^2\, s_a} \left(\frac{\pi^2 g_{*,R}}{90}\right)^{-1/4} \sqrt{\gamma_R(c_a)\, T_R\, M_{\rm pl}} \\ &\equiv \lambda_\gamma(T_R, c_a) \left(\frac{T_R}{10^{10}\,\text{GeV}}\right)^{1/2}\,. \end{aligned} \tag{S14}$$

This bound is illustrated in the right panel of Fig. S2. We see that we get the most conservative constraint by setting $s_a = 0$, for which we have $\lambda_\gamma(10^{10}\,\text{GeV}, 1) = 1.4 \times 10^{13}\,\text{GeV}$.

Couplings to Charged Matter

The calculation of the Goldstone production rates associated with the couplings to the SM fermions is somewhat less developed. In this section, we will calculate the relevant rates following the procedure outlined in [S3].

Preliminaries.—The integrated Boltzmann equation for the evolution of the number density of the Goldstone boson takes the form

$$\dot{n}_\phi + 3 H n_\phi = \Gamma(n_\phi^{\rm eq} - n_\phi)\,, \tag{S15}$$

where $n_\phi^{\rm eq} = \zeta(3)T^3/\pi^2$ is the equilibrium density of a relativistic scalar. In order to simplify the analysis, we will replace the integration over the phase space of the final states with the center-of-mass cross section, $\sigma_{\rm cm}$, or the center-of-mass decay rate, $\Gamma_{\rm cm}$. While this approach is not perfectly accurate, it has the advantage of relating the vacuum amplitudes to the thermal production rates in terms of relatively simple integrals.

For a two-to-two process, $1+2\to 3+4$, we have

$$\Gamma_{2\to2} \simeq \frac{1}{n_\phi^{\rm eq}} \int \frac{{\rm d}^3p_1}{(2\pi)^3}\frac{{\rm d}^3p_2}{(2\pi)^3}\frac{f_1(p_1)}{2E_1}\frac{f_2(p_2)}{2E_2} \times \big[1\pm f_3\big]\big[1\pm f_4\big]\, 2s\sigma_{\rm cm}(s)\,, \tag{S16}$$

where $f_{1,2}$ are the distribution functions of the initial states and $s\equiv(p_1+p_2)^2$ is the Mandelstam variable. We have included simplified Bose enhancement and Pauli blocking terms, $\big[1\pm f_3\big]\big[1\pm f_4\big] \to \frac{1}{2}\big([1\pm f_3(p_1)][1\pm f_4(p_2)] + \{p_1\leftrightarrow p_2\}\big)$, which is applicable in the center-of-mass frame where the initial and final momenta are all equal.[1] For $s\gg m_i^2$, the center-of-mass cross section is given by

$$\sigma_{\rm cm}(s) \simeq \frac{1}{32\pi}\int {\rm d}\cos\theta\, \frac{\sum|\mathcal{M}|^2(s,\theta)}{s}\,, \tag{S17}$$

where $\sum|\mathcal{M}|^2$ is the squared scattering amplitude including the sum over spins and charges and θ is the azimuthal angle in the center-of-mass frame. For all models of freeze-out considered in the main text, the center-of-mass cross section is independent of s. In this section, we will only encounter fermion-boson scattering or fermion annihilation. With the enhancement/blocking terms, one finds that the numerical pre-factors in both cases agree to within 10 percent. To simplify the calculations, we will therefore use the fermion annihilation rate throughout,

$$\Gamma_{2\to2} \simeq \sigma_{\rm cm}\, T^3 \left(\frac{7}{8}\right)^2 \frac{\zeta(3)}{\pi^2} \approx 0.093\,\sigma_{\rm cm}\, T^3\,. \tag{S18}$$

The advantage of this approach is that we can relate the center-of-mass cross section directly to the production rate with minimal effort and reasonable accuracy.

For a one-to-two process, $1\to2+3$, the decay rate in the center-of-mass frame is

$$\Gamma_{\rm cm} \simeq \frac{1}{32\pi\, m_1}\int {\rm d}\cos\theta\, \sum|\mathcal{M}|^2\,, \tag{S19}$$

where we have taken the two final particles to be massless. Since $\Gamma_{\rm cm}$ is independent of energy, the rate only depends on whether the initial state is a fermion or boson. Transforming this rate to a general frame gives

$$\Gamma_{1\to2} \simeq \frac{1}{n_\phi^{\rm eq}}\int\frac{{\rm d}^3p_1}{(2\pi)^3}\, f_1(p_1)\big[1\pm f_2(p_1/2)\big] \times\big[1\pm f_3(p_1/2)\big]\frac{m_1}{E_1}\Gamma_{\rm cm}\,, \tag{S20}$$

where f_1 is the distribution function of the decaying particle (not necessarily ϕ). We are mostly interested in the limit $T\gg m_1$, in which case the rate (S20) reduces to

$$\Gamma_{1\to2} \simeq \frac{m_1}{T}\frac{\pi^2}{16\zeta(3)}\,\Gamma_{\rm cm}\begin{cases} 1-\dfrac{4}{\pi^2} & \text{fermion,}\\[2ex] 1 & \text{boson,}\end{cases} \tag{S21}$$

where the dependence on the number of degrees of freedom of the decaying particle has been absorbed into $\Gamma_{\rm cm}$ through the sum over spins and charges. Note that, in equilibrium, the rates for decay and inverse decay are equal.

Coupling to charged fermions.—We consider the following coupling between a Goldstone boson and charged fermions:

$$\mathcal{L}_{\phi\psi} = \frac{\phi}{\Lambda_\psi}\left({\rm i}H\,\bar\psi_{L,i}\,g^{ij}\,\psi_{R,j} + {\rm h.c.}\right), \tag{S22}$$

where $g^{ij}\equiv[(\lambda_i-\lambda_j)g_V^{ij}+(\lambda_i+\lambda_j)g_A^{ij}]$, H is the Higgs doublet, $\psi_{L,R}\equiv\frac{1}{2}(1\mp\gamma^5)\psi$, and the $SU(2)_L$ and $SU(3)_c$ structures have been left implicit. Distinct processes dominate in the various limits of interest.

- At high energies, the Goldstone boson is produced through the following two processes (see Fig. S3): (a) $\psi_i+\bar\psi_j\to H+\phi$ and (b) $\psi_i+H\to\psi_j+\phi$. Summing over the spins and charges, we get

$$\sum|\mathcal{M}|^2_{(a)} = 4N_\psi\, s\, g(\lambda_i, g_I^{ij})\,, \tag{S23}$$

$$\sum|\mathcal{M}|^2_{(b)} = 4N_\psi\, s(1-\cos\theta)\, g(\lambda_i, g_I^{ij})\,, \tag{S24}$$

where

$$g(\lambda_i, g_I^{ij}) \equiv \frac{(\lambda_i-\lambda_j)^2(g_V^{ij})^2+(\lambda_i+\lambda_j)^2(g_A^{ij})^2}{\Lambda_\psi^2}\,, \tag{S25}$$

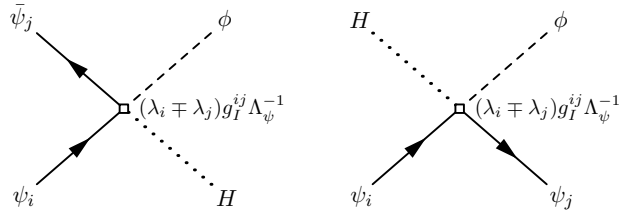

(a) Fermion annihilation. (b) Fermion-Higgs scattering.

Figure S3. Feynman diagrams for the dominant Goldstone production via the coupling to charged fermions above the electroweak scale. For the vector and axial vector couplings, $I\in\{V,A\}$, the "−" and "+" signs apply, respectively.

[1] These Pauli blocking and Bose enhancement terms were not included in [S3], as they complicate the rate calculations. We have included them to ensure that the rates computed for both the forward and backward processes give the same results.

and we have combined fermion and anti-fermion scattering in the sum over charges as well as introduced

$$N_\psi \equiv \begin{cases} 1 & \psi = \text{lepton}, \\ 3 & \psi = \text{quark}. \end{cases} \tag{S26}$$

We also find it convenient to define $\Lambda^I_{ij} \equiv \Lambda_\psi / g^{ij}_I$, with $I \in \{V, A\}$. Using (S17) and (S18), and treating the vector and axial-vector couplings separately, we find

$$\begin{aligned} \Gamma^I_{ij} &= N_\psi \left(\frac{7}{8}\right)^2 \frac{4\zeta(3)}{\pi^2} \frac{(\lambda_i \mp \lambda_j)^2}{8\pi} \frac{T^3}{(\Lambda^I_{ij})^2} \\ &\simeq 0.19\, N_\psi \frac{(\lambda_i \mp \lambda_j)^2}{8\pi} \frac{T^3}{(\Lambda^I_{ij})^2}\,, \end{aligned} \tag{S27}$$

where the "−" and "+" signs apply to $I = V$ and $I = A$, respectively.

• Below the scale of EWSB (which is the regime most relevant for the freeze-in constraints), the Lagrangian (S22) becomes

$$\begin{aligned} \mathcal{L}_{\phi\psi} \;=\; & \mathrm{i}\frac{\phi}{\Lambda_\psi} \bar\psi_i \Big[(m_i - m_j) g_V^{ij} \\ & + (m_i + m_j) g_A^{ij} \gamma^5 \Big] \psi_j \,, \end{aligned} \tag{S28}$$

where $m_i \equiv \sqrt{2}\lambda_i / v$. The Goldstone production processes associated with these couplings are shown in Fig. S4.

We first consider the diagonal part of the interaction, which takes the form $\mathrm{i}\tilde\epsilon_{ii}\, \phi \bar\psi_i \gamma^5 \psi_i$, with $\tilde\epsilon_{ii} \equiv 2 m_i g_A^{ii} / \Lambda_\psi$. Kinematical constraints require us to include at least one additional particle in order to get a non-zero amplitude. The two leading processes are (*a*) $\psi_i + \{\gamma, g\} \to \psi_i + \phi$ (cf. Fig. S4a) and (*b*) $\psi_i + \bar\psi_i \to \phi + \{\gamma, g\}$ (cf. Fig. S4b), where $\{\gamma, g\}$ is either a photon or gluon depending on whether the fermion is a lepton or quark, respectively. Summing over spins and charges, we obtain

$$\sum |\mathcal{M}|^2_{(a)} = 16\pi\, A_\psi\, |\tilde\epsilon_{ii}|^2 \frac{s^2}{(m_i^2 - t)(m_i^2 - u)}\,, \tag{S29}$$

$$\sum |\mathcal{M}|^2_{(b)} = 16\pi\, A_\psi\, |\tilde\epsilon_{ii}|^2 \frac{t^2}{(s - m_i^2)(m_i^2 - u)}\,, \tag{S30}$$

where s, t and u are the Mandelstam variables and

$$A_\psi \equiv \begin{cases} \alpha & \psi = \text{lepton}, \\ 4\alpha_s & \psi = \text{quark}. \end{cases} \tag{S31}$$

In the massless limit, the cross section has IR divergences in the t- and u-channels from the exchange of a massless fermion. The precise production rate therefore depends on the treatment of the soft modes. Regulating the IR divergence with the fermion mass and taking the limit $s \gg m_i^2$, we find

$$\sigma_{\rm cm}(s) \simeq \frac{1}{s}\, A_\psi\, |\tilde\epsilon_{ii}|^2 \left[3 \log \frac{s}{m_i^2} - \frac{3}{2} \right]. \tag{S32}$$

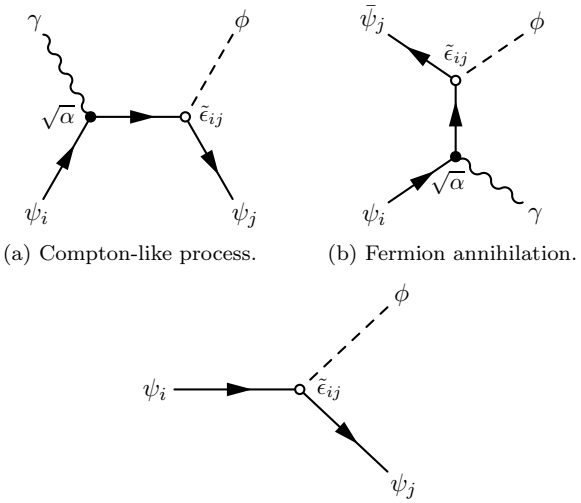

(a) Compton-like process. (b) Fermion annihilation.

(c) Fermion decay.

Figure S4. Feynman diagrams for the dominant Goldstone production via the coupling to charged fermions below the electroweak scale. For quarks, the coupling to photons is replaced by that to gluons. In addition to the displayed s- and t-channel diagrams for the Compton-like process and fermion annihilation, there are u-channel diagrams which are not shown.

At high temperatures, the fermion mass is controlled by the thermal mass $m_i^2 \to m_T^2 = \frac{1}{2}\pi A_\psi T^2$ and the production rate becomes

$$\tilde\Gamma_{ii} = \frac{3\pi^3}{64\zeta(3)} A_\psi \frac{|\tilde\epsilon_{ii}|^2}{8\pi} T \left[\log \frac{2}{\pi A_\psi} + 2\log 2 - \frac{3}{2} \right]. \tag{S33}$$

This formula is expected to break down at $T \lesssim m_i$, but will be sufficient at the level of approximation being used in this paper. A proper treatment of freeze-in at $T \sim m_i$ should go beyond $\Gamma = H$ and fully solve the Boltzmann equations. However, this level of accuracy isn't needed for estimating the constraint on the coupling $\tilde\epsilon_{ii}$.

The result (S33) will be of limited utility for the coupling to quarks. This is because, for $T \lesssim 30\,\text{GeV}$, the QCD coupling becomes large and our perturbative calculation becomes unreliable.[2] In fact, we see that the production rate (S33) becomes negative in this regime. While the top quark is sufficiently heavy to be still at weak coupling, its mass is close to the electroweak phase transition and, therefore, the assumption $s \gg m_t^2$ is not applicable. For these reasons, we will not derive bounds on the quark couplings from these production rates.

When the coupling of ϕ is off-diagonal in the mass basis, the dominant process at low energies is the decay $\psi_i \to \psi_j + \phi$, cf. Fig. S4c. Since the mass splittings of the

[2] These effects are computable using the techniques of [S5], but this is beyond the scope of the present work.

SM fermions are large and $m_\phi \ll m_\psi$, the center-of-mass decay rate is well approximated by

$$\Gamma_{\rm cm} = \frac{N_\psi}{8\pi}\frac{m_i^3}{\Lambda_{ij}^2}\,, \tag{S34}$$

where $\Lambda_{ij} \equiv \left[(g_V^{ij})^2 + (g_A^{ij})^2\right]^{-1/2}\Lambda_\psi$. Using (S21), we get

$$\tilde{\Gamma}_{ij} = \frac{(\pi^2-4)}{16\zeta(3)}\frac{N_\psi}{8\pi}\frac{1}{T}\frac{m_i^4}{\Lambda_{ij}^2} \simeq 0.31 N_\psi \frac{|\tilde{\epsilon}_{ij}|^2}{8\pi}\frac{m_i^2}{T}\,, \tag{S35}$$

with $\tilde{\epsilon}_{ij} \approx m_i/\Lambda_{ij}$. In addition to this decay, we also have production with a photon or gluon, given by (S33) with $\tilde{\epsilon}_{ii} \to \tilde{\epsilon}_{ij}$. We will neglect this contribution as it is suppressed by a factor of α or α_s for $T \sim m_i$.

COMMENTS ON DECAYS

We have treated each of the operators which couple the pNGBs to the SM independently throughout. For computing the production rates, this is justified since the amplitudes for the different processes that we consider do not interfere and the couplings therefore add in quadrature. One may still ask, however, if the interplay between several operators can affect the cosmological evolution after the production. In particular, one might worry that some operators would allow for the decay of the pNGBs and that this might evade the limits on $N_{\rm eff}$. In this part, we will address this concern. We are assuming that $m_\phi < 1\,\text{MeV}$, so that the only kinematically allowed decays are to photons and neutrinos.

Decay to Photons

The coupling $\phi F\tilde{F}$ can mediate the decay of axions to photons. However, for the range of parameters of interest, these decays occur after recombination and, hence, do not affect the CMB. To see this, we consider the decay rate for $m_\phi \gtrsim T$ [S6],

$$\Gamma_{D,\gamma} = \frac{1}{64\pi}\frac{m_\phi^3}{\Lambda_\gamma^2}\,. \tag{S36}$$

The decay time is $\tau_D = \Gamma_{D,\gamma}^{-1}$ and the temperature at decay is determined by $H(T_D) \approx \tau_D^{-1} = \Gamma_{D,\gamma}$. We will not consider the regime $m_\phi < T_D$ as it does not arise in the range of parameters of interest. Assuming that the universe is matter dominated at the time of the decay, we get

$$\frac{T_D}{T_{\rm rec}} \approx 9.5\times 10^{-10}\left(\frac{\Lambda_\gamma}{10^{10}\,\text{GeV}}\right)^{-4/3}\left(\frac{m_\phi}{T_{\rm rec}}\right)^2\,. \tag{S37}$$

Recalling the constraint from stellar cooling, $\Lambda_\gamma > 1.3\times 10^{10}\,\text{GeV}$ [S7], we therefore infer that $T_D < 7.1\times 10^{-10}\,T_{\rm rec}\,(m_\phi/T_{\rm rec})^2$, so that the axions are stable on the time-scale of recombination as long as $m_\phi \lesssim 10\,\text{keV}$. CMB-S4 will probe this regime through sensitivity to $N_{\rm eff}$ for $m_\phi \lesssim T_{\rm rec}$ and through sensitivity to warm dark matter for larger masses. Warm dark matter is already highly constrained by cosmology, with values of m_ϕ above 1 eV typically ruled out by the CMB. For comparison, a stable particle with $m_\phi \gtrsim 100\,\text{eV}$ produces $\Omega_m > 1$ and is therefore excluded by constraints on the dark matter abundance. For $m_\phi > 10\,\text{keV}$, the decay to photons does affect the phenomenology and must be considered explicitly. Nevertheless, in the regime of interest, $10\,\text{keV} < m_\phi < 1\,\text{MeV}$ (where the axion decays between neutrino decoupling and recombination), the pNGBs are non-relativistic and, therefore, carry a large energy density, $\rho_\phi \simeq m_\phi n_\phi$. As a result, this region is highly constrained by current cosmological observations [S8, S9].

Decay to Neutrinos

Depending on the mass of the pNGB, the decay to neutrinos leads to the following three scenarios:

- For $m_\phi < T_{\rm rec}$, the strong interactions between the pNGBs and the neutrinos imply that the neutrinos are no longer free-streaming particles [S10–S12], which is ruled out by recent CMB observations [S13].

- For $T_D > m_\phi > T_{\rm rec}$, the pNGBs are brought into equilibrium with the neutrinos at $T \sim T_D$ and then become Boltzmann suppressed for $T \lesssim m_\phi$. This process leads to a contribution to $N_{\rm eff}$, even if the pNGBs have negligible energy density to begin with. To estimate the size of the effect, we first note that the freeze-in at T_D conserves the total energy density in neutrinos and pNGBs,

$$(g_\nu + g_\phi)(a_1 T_1)^4 = g_\nu (a_0 T_0)^4\,, \tag{S38}$$

where T_0 and T_1 are the initial and final temperatures during the equilibration, and g_ν and $g_\phi = 1$ are the effective numbers of degrees of freedom in ν and ϕ, respectively. When the temperature drops below the mass of the pNGBs, their energy density is converted to neutrinos. This process conserves the comoving entropy density,

$$(g_\nu + g_\phi)(a_1 T_1)^3 = g_\nu (a_2 T_2)^3\,, \tag{S39}$$

where $T_2 \ll m_\phi$ is some temperature after the pNGB population has decayed. The final energy density of the neutrinos becomes

$$a_2^4 \rho_{\nu,2} = \left(\frac{g_\nu + g_\phi}{g_\nu}\right)^{1/3} a_0^4 \rho_{\nu,0}\,, \tag{S40}$$

where $\rho_{\nu,i} \equiv \rho_\nu(a_i)$. Using the definition of $N_{\rm eff}$ in (2) of

the main text and $a^4\rho_\gamma = const.$, we find

$$N_{\rm eff} = \left(\frac{g_\nu + g_\phi}{g_\nu}\right)^{1/3} N_{\rm eff,0}\,. \tag{S41}$$

Considering the coupling to a single neutrino flavor (rather than all three), i.e. $N_{\rm eff,0} \simeq 1$ and $g_\nu = 7/4$, we then get

$$\Delta N_{\rm eff} = \left(1 + \frac{4}{7}\right)^{1/3} - 1 \simeq 0.16\,, \tag{S42}$$

where $\Delta N_{\rm eff} \equiv N_{\rm eff} - N_{\rm eff,0}$. Coupling to more than one neutrino flavor and including a non-zero initial temperature for the pNGBs would increase this number slightly, so that we will use $\Delta N_{\rm eff} \geq 0.16$.

• The production of pNGBs through the freeze-in process is avoided if $m_\phi > T_D > T_{\rm rec}$, in which case the pNGBs decay to neutrinos out of equilibrium. To a good approximation, this decay conserves the energy density, which is therefore simply transferred from ϕ to ν at the time of the decay. The contribution to $\Delta N_{\rm eff}$ is enhanced by the amount of time that ϕ is non-relativistic before its decay, which may be a large effect for $m_\phi \gg 1\,{\rm eV}$.

In summary, operators that allow the Goldstone bosons to decay do not substantially alter the predictions presented in the main text. On the one hand, decays to photons cannot occur early enough to impact the CMB. On the other hand, decays to neutrinos typically increase the contributions to $\Delta N_{\rm eff}$ and would therefore strengthen our bounds.

[S1] E. Braaten and T. Yuan, Phys. Rev. Lett. **66**, 2183 (1991).

[S2] M. Bolz, A. Brandenburg, and W. Buchmüller, Nucl. Phys. B **606**, 518 (2001).

[S3] E. Masso, F. Rota, and G. Zsembinszki, Phys. Rev. D **66**, 023004 (2002).

[S4] P. Graf and F. Steffen, Phys. Rev. D **83**, 075011 (2011).

[S5] A. Salvio, A. Strumia, and W. Xue, J. Cosmol. Astropart. Phys. **1401**, 011 (2014).

[S6] M. Peskin and D. Schroeder, *An Introduction to Quantum Field Theory* (Addison-Wesley, Reading, MA, 1995).

[S7] A. Friedland, M. Giannotti, and M. Wise, Phys. Rev. Lett. **110**, 061101 (2013).

[S8] D. Cadamuro and J. Redondo, J. Cosmol. Astropart. Phys. **1202**, 032 (2012).

[S9] M. Millea, L. Knox, and B. Fields, Phys. Rev. D **92**, 023010 (2015).

[S10] Z. Chacko, L. Hall, T. Okui, and S. Oliver, Phys. Rev. D **70**, 085008 (2004).

[S11] S. Hannestad and G. Raffelt, Phys. Rev. D **72**, 103514 (2005).

[S12] A. Friedland, K. Zurek, and S. Bashinsky, arXiv:0704.3271 [astro-ph].

[S13] D. Baumann, D. Green, J. Meyers, and B. Wallisch, J. Cosmol. Astropart. Phys. **1601**, 007 (2016).